

## Structural and optical properties of a NaCl single crystal doped with CuO nanocrystals

This content has been downloaded from IOPscience. Please scroll down to see the full text.

2013 Chinese Phys. B 22 098103

(<http://iopscience.iop.org/1674-1056/22/9/098103>)

View [the table of contents for this issue](#), or go to the [journal homepage](#) for more

Download details:

IP Address: 137.99.31.134

This content was downloaded on 20/05/2015 at 02:12

Please note that [terms and conditions apply](#).

# Structural and optical properties of a NaCl single crystal doped with CuO nanocrystals\*

S. Addala<sup>a)</sup>, L. Bouhdjer<sup>a)†</sup>, A. Chala<sup>b)</sup>, A. Bouhdjar<sup>b)</sup>, O. Halimi<sup>a)</sup>, B. Boudine<sup>a)</sup>, and M. Sebais<sup>a)</sup>

<sup>a)</sup>Laboratory of Crystallography, Department of Physics, Mentouri University of Constantine, Constantine 25000, Algeria

<sup>b)</sup>Laboratory of Applied Chemistry, Department of Physics, Mohamed Khaider University of Biskra, Biskra 07000, Algeria

(Received 22 July 2012; revised manuscript received 4 March 2013)

A cupric oxide (CuO) nanocrystal-doped NaCl single crystal and a pure NaCl single crystal are grown by using the Czochralski (Cz) method. A number of techniques, including X-ray diffraction (XRD), scanning electron microscopy (SEM), energy dispersive X-ray (EDX) analysis, Fourier transform infrared (FT-IR) spectroscopy, Raman spectroscopy, optical absorption in the UV–visible range, and photoluminescence (PL) spectroscopy are used to characterize the obtained NaCl and NaCl:CuO crystals. It is observed that the average radius of CuO crystallites in NaCl:CuO crystal is about 29.87 nm, as derived from the XRD data analysis. Moreover, FT-IR and Raman spectroscopy results confirm the existence of the monoclinic CuO phase in NaCl crystal. UV–visible absorption measurements indicate that the band gap of the NaCl:CuO crystal is 434 nm (2.85 eV), and it shows a significant amount of blue-shift ( $\Delta E_g = 1$  eV) in the band gap energy of CuO, which is due to the quantum confinement effect exerted by the CuO nanocrystals. The PL spectrum of the NaCl:CuO shows a broad emission band centred at around 438 nm, which is consistent with the absorption measurement.

**Keywords:** NaCl single crystal, CuO nanocrystals, Raman spectroscopy, photoluminescence

**PACS:** 81.10.–h

**DOI:** 10.1088/1674-1056/22/9/098103

## 1. Introduction

Recently, interesting optical, electronic, and magnetic size-dependent properties of semiconductor nanocrystals have attracted extensive attention, not only because of their quantum-confinement effects, which are very important for the research of the fundamental physical properties depending on dimensionality, but also because of their potential applications in nano-electronics and nanodevices. Among the nanosemiconductors, cupric oxide (CuO) has attracted increasing interest for both fundamental and practical reasons. It can be widely used in applications such as gas sensors, magnetic storage medium, electronics, solar-energy transformation, semiconductors, catalysis,<sup>[1–4]</sup> high- $T_c$  superconductors,<sup>[5]</sup> and field emission (FE) emitters.<sup>[6–9]</sup> CuO is a p-type semiconductor with a narrow bandgap. It has been studied together with the other copper oxides, especially on its applications as a photothermally active and photoconductive compound. The study of the optical properties of semiconductor nano-crystals (NCs) in ionic solids can be very conveniently carried out on the simplest compound alkali halides AX, where A denotes an alkali cation and X a halogen anion. They offer a number of advantages such as simple structure, high degree of chemical purity, easy manipulation, and wide range of possible doping impurities with different concentrations. On the other hand, their high gap energy ( $\sim 10$  eV) provides a large window for optical spectroscopy studies. In addition, their diamagnetism and their high electrical resistance allow the convenient use of

spin resonance methods. There are several studies addressing optical properties of alkali halide single crystals doped with nano-crystals of semiconductors, such as NaCl:CuCl, KCl:AgCl, KBr:ZnO, NaCl:CdS, and KBr:CdTe.<sup>[10–16]</sup> In addition, recently, a great number of studies have been stimulated by alkali halides doped with metal ions like KCl:Ag, KCl:Au, NaCl:Cu, and KCl:Cu.<sup>[17–19]</sup> In the present paper, we investigate the doping effects of CuO nanocrystals on the structural and optical properties of the NaCl single crystals experimentally.

## 2. Experimental details

NaCl and NaCl:CuO were prepared using the Czochralski (Cz) method. A given weight of NaCl powder was mixed with 2 wt% CuO nanopowder, and this mixture was heated in a crucible until they fused. The oven temperature was controlled using a [REX-C100 SEPIES] controller and a platinum/platinum radium (10%) thermocouple. The pulling rate was in a range of 8–10 mm/h and a rotation speed of about  $V_r = 1$  rpm was used along the part (a) and  $V_r = 0$  rpm along the part (b) of NaCl:CuO crystal (see Fig. 1). As is well known, crystal rotation is a dominant factor influencing the crystal-melt interface.<sup>[20]</sup> In general, crystal rotation during the Cz growth is mainly used to provide a symmetric temperature profile. The last factor has a direct effect on the diameter of the crystal as indicated in Fig. 1. The growth is carried out following the crystallographic  $\langle 100 \rangle$  axis. The obtained crystals

\*Project supported by the Crystallography Laboratory of the University of Constantine, Algeria.

†Corresponding author. E-mail: bouhdjerlazhar@gmail.com

are cleaved into samples, each with face being parallel to the (100) plane.

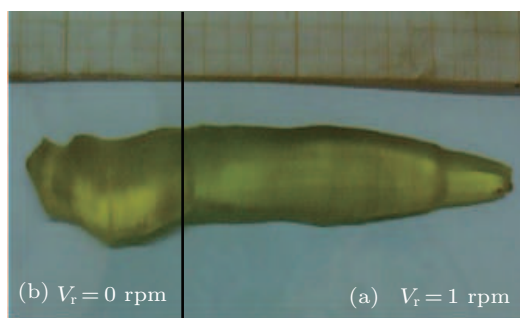


Fig. 1. (color online) Photograph of a NaCl:CuO single crystal.

XRD data were obtained using the Cu  $K_{\alpha}$  radiation ( $\lambda_{K\alpha} = 1.5402 \text{ \AA}$ ) and a graphite filter in a BRUKER-AXS D8 diffractometer. The structural analyses of NaCl and NaCl:CuO samples were carried out using a (Jobin–Yvon)  $\mu$ -Raman spectrometer at room temperature (RT). The FT-IR investigation was performed with Thermo-Nicolet equipment in the  $4000\text{--}400 \text{ cm}^{-1}$  range. For oxides, all bands have characteristic frequencies between  $1000 \text{ cm}^{-1}$  and  $400 \text{ cm}^{-1}$ . Optical properties were studied using a UV–visible spectrophotometer (Shimadzu, UV-3101). Furthermore, the PL was measured at RT and the samples were excited by an argon laser (ionized light  $E_{\text{exc}} = 313 \text{ nm}$ ) with an output power of 10 mW.

### 3. Results and discussion

XRD studies have been performed on samples of pure NaCl and NaCl:CuO crystals to determine their crystallographic structure.

Figure 2 shows the XRD spectrum of a pure NaCl single crystal, which exhibits two intense peaks located at  $2\theta = 31.73^{\circ}$  and  $2\theta = 66.34^{\circ}$ . These two peaks correspond respectively to the (200) plane and its harmonic (400). This result indicates that pure NaCl crystallized in the cubic system with the  $Fm\bar{3}m$  symmetry space group as reported in the JCPDS 05-0628 card. In addition, it indicates that the sample has a single-crystal character, and confirms that the crystal is cleaved in the direction parallel to the (100) plane.

The XRD spectrum of the CuO nanopowder is presented in Fig. 3. The diffraction peaks are easily indexed as being consistent with the monoclinic structure of CuO with lattice constants  $a = 4.69$ ,  $b = 3.42$ ,  $c = 5.13 \text{ \AA}$ ,  $\beta = 99^{\circ}52'$ , and the  $C2/c$  symmetry space group as reported in the JCPDS 41-0254 card. The broadening of the major peaks indicates the nanometric particle size, which is found to be about 15.5 nm. The crystallite size of CuO is estimated using Scherrer's formula<sup>[21]</sup>

$$D = \frac{0.9\lambda}{B(\theta)\cos(\theta)}, \quad (1)$$

where  $D$  is the crystallite diameter,  $\lambda$  the wavelength,  $\theta$  the Bragg angle, and  $B(\theta)$  the full width at half maximum (FWHM) of the peak.

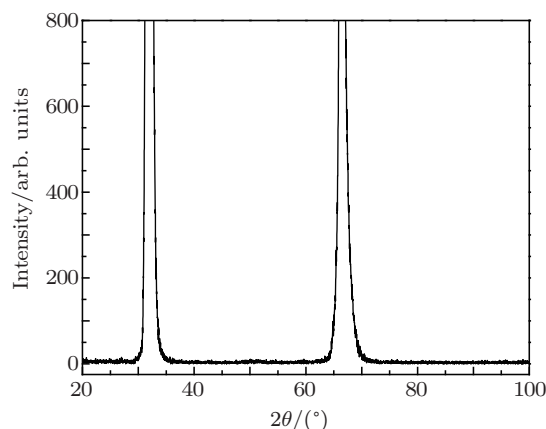


Fig. 2. XRD pattern of a pure NaCl single crystal (faces are parallel to the (100) plane).

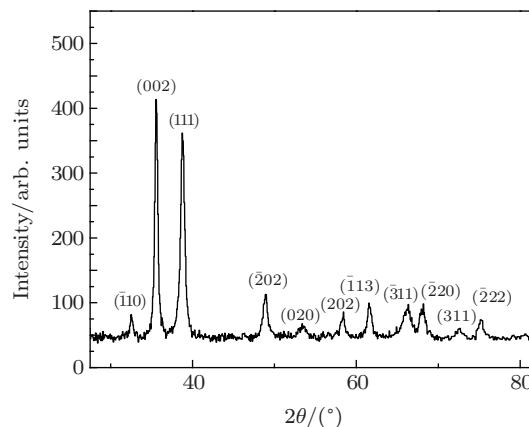


Fig. 3. XRD pattern of the CuO nanopowder.

In Fig. 4, the typical XRD pattern of the NaCl:CuO sample is displayed. Besides the peaks related to the host (NaCl), there are two peaks located at  $2\theta = 35.60^{\circ}$  and  $2\theta = 59.13^{\circ}$ , attributed to the CuO phase. The significant intensities of these peaks indicate the high crystalline quality of CuO NCs. However, the other peaks of CuO are not visible, and this observation indicates that the crystallites of CuO display preferred growth in these two directions. Fröhlich *et al.*<sup>[10]</sup> have already proved that the axes of CuCl NCs are parallel to the axes of the NaCl lattice. On the other hand, this result demonstrates the incorporation of CuO NCs into the NaCl host and the absence of peaks corresponding to other phases, such as CuCl, indicating that there is no chemical reaction between CuO and NaCl, in spite of the high temperature of preparation. However, the size of CuO NCs embedded in NaCl is almost doubled (29.87 nm) as compared with that of CuO nanopowder. We speculate that available conditions in environment of crystal growth contribute to the growth process of CuO NCs. Table 1

presents the average sizes of the crystallites corresponding to each diffracting plane. The average radius is about 29.87 nm.

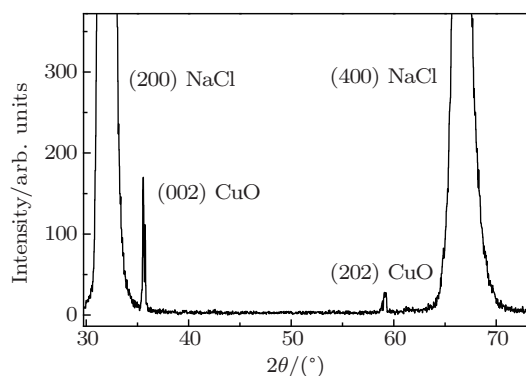


Fig. 4. XRD pattern of a NaCl:CuO crystal.

Figure 5 displays an SEM micrograph of a NaCl:CuO crystal. It exhibits a quasi-spherical shape of CuO crystallites scattered on the surface of NaCl. The mean crystallite size obtained using Scherrer's formula is in all cases substantially smaller than the dimension of the grain observed by the SEM image, indicating that these grains are probably aggregates of many crystallites of CuO. The Gibbs free energy of the surface of NCs is usually high, and the NCs have the tendency toward aggregate formation, thereby reducing the Gibbs free energy of the surface.<sup>[22]</sup>

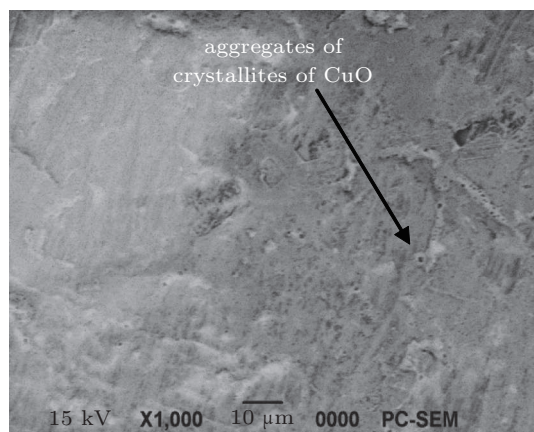


Fig. 5. SEM micrograph of a NaCl:CuO crystal.

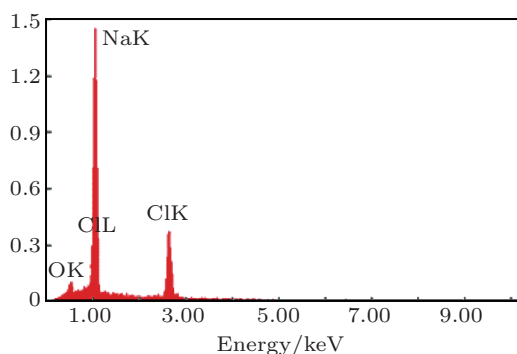


Fig. 6. (color online) Typical EDX pattern of a NaCl:CuO single crystal.

The energy dispersive X-ray analysis (EDX) spectrum (see Fig. 6) indicates the presence of Na, Cl, Cu, and O elements, but the absence of other elements, demonstrating that the NaCl:CuO single crystal has a very high purity.

Table 1. Crystallite sizes calculated from the XRD pattern.

$2\theta/(\circ)$	FWHM/ $(\circ)$	$(hkl)$	$D/\text{nm}$
35.60	0.262	(0 0 2)	32.08
59.13	0.332	(2 0 2)	27.67

Raman spectroscopy, which is sensitive to the local atomic arrangements and the vibrations of the material, has been widely used to investigate the structures of nano-sized materials.<sup>[23,24]</sup> Figure 7 shows the Raman spectrum of NaCl:CuO at RT. It can be seen from XRD patterns that the CuO NCs have a monoclinic structure, which belongs to the  $C2/c$  space group with two molecules per unit cell. There are three Raman modes  $1A_g+2B_g$ .<sup>[25,26]</sup> It can be seen from the spectrum that there are three Raman peaks located at 283, 338, and  $647\text{ cm}^{-1}$ , respectively. The peak at  $283\text{ cm}^{-1}$  can be assigned to the  $A_g$  mode, while the peaks at 338 and  $647\text{ cm}^{-1}$  can be ascribed to the  $B_g$  mode. On the other hand, the Raman spectra of CuO nanopowder reported by Wang *et al.*<sup>[27]</sup> and Dar *et al.*<sup>[28]</sup> exhibit that the intensity of the  $A_g$  mode is more intense than those of the  $2B_g$  modes. In contrast, the Raman spectrum in this study shows that the  $B_g$  mode located at around  $338\text{ cm}^{-1}$  has the strongest intensity. This result may be attributed to the constraints exerted by the NaCl matrix on the CuO NCs.

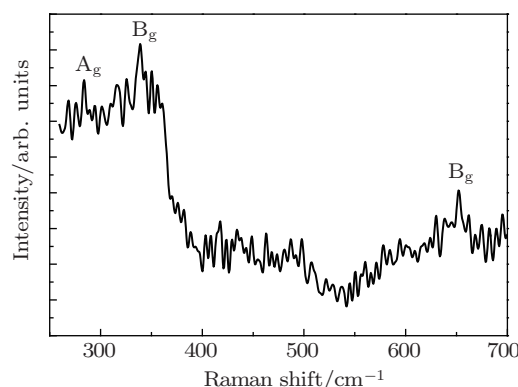


Fig. 7. Raman spectrum of NaCl:CuO.

Figure 8 displays the FT-IR transmission spectra of NaCl and NaCl:CuO crystals. As is well known, the alkali halides are transparent in the IR range, and Fig. 8(a) exhibits this property clearly. However, the FT-IR spectrum of NaCl:CuO in Fig. 8(b) shows four peaks located, respectively, at 437, 485, 546, and  $605\text{ cm}^{-1}$  which are characteristics of vibrations along the Cu–O bond.<sup>[29,30]</sup> These results confirm the inclusion of the CuO phase in the NaCl host.

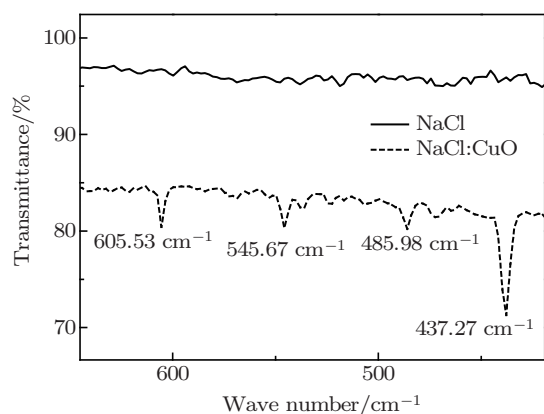


Fig. 8. FT-IR spectra of pure NaCl and NaCl:CuO.

The optical absorption spectrum of a pure NaCl crystal, represented in Fig. 9(a), shows that NaCl is transparent in the visible region and has a strong absorption near ultraviolet, and the optical band gap determined by the second derivative method<sup>[31]</sup> is  $E_{g\text{NaCl}} = 6.42$  eV (see Fig. 9(b)). On the other hand, Fig. 10(a) shows the optical absorption spectrum of NaCl:CuO, displaying a broad absorption peak centred at 434 nm (2.85 eV, see Fig. 10(b)) relative to the allowed direct transitions which are dominant in the CuO NCs. This band gap energy is consistent with the figure of 2.9 eV reported by Maji *et al.*<sup>[32]</sup> for the CuO nanocrystals having a size of 20 nm. As given by Santra *et al.*,<sup>[33]</sup> the monoclinic CuO bulk crystal has a band gap energy of 1.85 eV, so CuO NCs has a blue-shift of their absorption edge ( $\Delta E_{g\text{CuO}} = 1$  eV). This blue-shift is caused by the well-known quantum confinement effect. The Bohr radius of CuO semiconductor is 28.27 nm.<sup>[34]</sup> However, even in the case where the confinement length ( $D = 29.87$  nm) is larger than the Bohr radius, there are interesting effects due to the confinement of translational motion of the whole exciton.

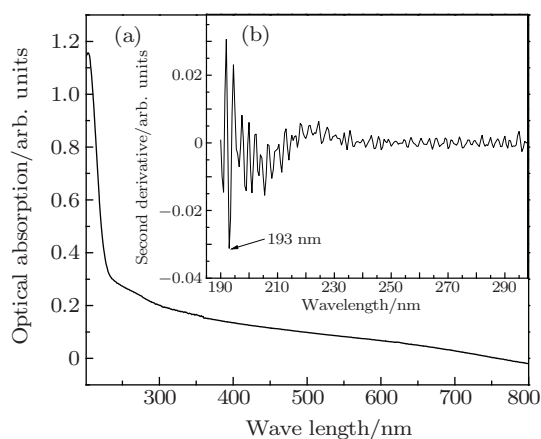


Fig. 9. (a) Optical absorption spectrum of the pure NaCl crystal and (b)  $E_g$  of the NaCl crystal, determined by the second derivative.

Figure 11 displays the PL spectrum of NaCl:CuO at RT. It shows a broad emission band centred at 438 nm (2.83 eV) with

a blue-shift  $\Delta E_g = 0.98$  eV, which is in consistency with the optical absorption measurement. A similar result is obtained by Maji *et al.*<sup>[32]</sup> who observed an emission band centred at 406 nm for a CuO nanocrystal size of 20 nm when the excitation wavelength was 325 nm. Moreover, the strong PL intensity from the CuO NCs embedded in NaCl can be attributed to their high crystallization and to their good surface, which is in agreement with the XRD patterns of NaCl:CuO discussed earlier. In addition, the NaCl single crystal is a suitable host for studying the optical properties of CuO NCs in the UV-visible range.

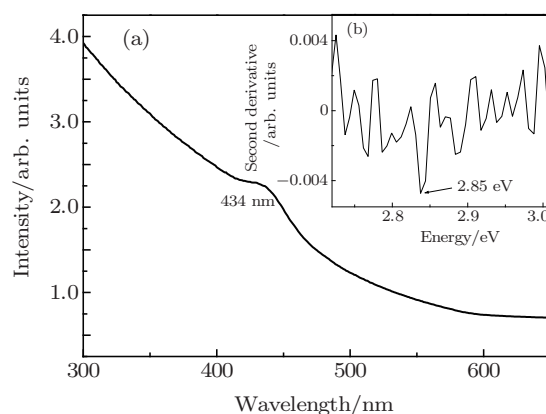


Fig. 10. (a) Optical absorption spectrum of an NaCl:CuO crystal and (b)  $E_g$  of CuO NCs determined by the second derivative.

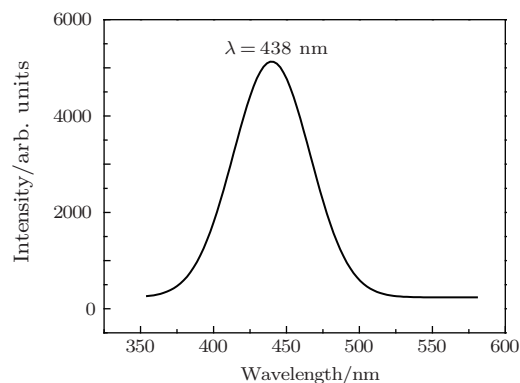


Fig. 11. Photoluminescence spectrum of an NaCl:CuO crystal.

#### 4. Conclusions

In this paper, NaCl and NaCl:CuO crystals are successfully grown by the Cz method. Structural characterization by XRD confirms the incorporation of monoclinic CuO NCs into the NaCl host which retains its monocrystalline character. Furthermore, the SEM image presents large quasi-spherical particles of the CuO NCs and the EDX analyses indicate the high purity of the NaCl:CuO single crystal. On the other hand, Raman and FT-IR spectra verify the Cu–O vibration mode. In addition, the optical absorption exhibits a broadband that indicates a size distribution and a blue-shift of the absorption edge

compared with that from the bulk CuO. The PL spectrum at RT shows a blue luminescence band located at 438 nm with a shift toward the short wavelength. This blue-shift is due to the quantum confinement effects of charges in CuO NCs.

## Acknowledgment

The authors thank Prof. A. B. Chala for his assistance.

## References

- [1] Frietsch M, Zudock F, Goschnick J and Bruns M 2000 *Sensor. Actuators. B* **65** 379
- [2] Maruyama T 1998 *Sol. Energy Mater. Solar Cells* **56** 85
- [3] Jiang Y, Decker S, Mohs C and Klabunde K J 1998 *Catalysis* **180** 24
- [4] Ao B, Kummerl L and Haarer K 1995 *Adv. Mater.* **7** 495
- [5] Muller K H 2001 *High- $T_c$  Superconductors and Related Materials* (Dordrecht: Kluwer Academic)
- [6] Chen J, Deng S, Xu N, Zhang W, Wen X and Yang S 2003 *Appl. Phys. Lett.* **83** 746
- [7] Yeon S C, Sung W Y, Kim W J, Lee S M, Lee H Y, Kim Y H and Vac J 2006 *Sci. Technol. B* **24** 940
- [8] Hsieh C T, Chen J M, Lin H H and Shih H C 2003 *Appl. Phys. Lett.* **83** 3383
- [9] Zhu Y W, Yu T, Cheong F C, Xu X J, Lim C T, Tan V B C, Thong J T L and Sow C H 2005 *Nanotechnology* **16** 88
- [10] Fröhlich D, Haselhoff M and Reimann K 1995 *Solid State Commun.* **94** 189
- [11] Haselhoff M and Weber H J 1998 *Phys. Rev. B* **58** 5052
- [12] Vogelsang H, Husberg O, Köhler U and Von der Osten W 2000 *Phys. Rev. B* **61** 1874
- [13] Baranov P G, Romanov N G, Khramtsov V A and Vikhnin V S 2001 *J. Phys.: Condens. Matter* **13** 2651
- [14] Halimi O, Boudine B, Sebais M, Challouche A, Mouras R and Boudrioua A 2003 *Mater. Sci. Eng. C* **23** 1111
- [15] Boudine B, Sebais M, Halimi O, Alliouche H, Boudrioua A and Mouras R 2004 *Catal. Today* **89** 293
- [16] Bensouici A, Plaza J L, Diéguez E, Halimi O, Boudine B, Addala S, Guerbous L and Sebais M 2009 *Luminescence* **129** 948
- [17] Taketashi K and Takeshi H 2012 *Luminescence* **132** 513
- [18] Sung M K, Gwang S K and Sang Y L 2008 *Mater. Lett.* **62** 4354
- [19] Daniel D J, Ramasamy P, Madhusoodanan U and Bhagavannarayana G 2012 *J. Cryst. Growth* **353** 95
- [20] Seung-Suk S and Kyung-Woo Y 2005 *J. Cryst. Growth* **275** e249
- [21] Cullity B D 1978 *Elements of X-Ray Diffraction* (2nd edn.) (Reading, MA: Addison-Wesley) p. 102
- [22] Zhu J, Chan H, Liu H, Yang X, Lu L and Wang X 2004 *Mater. Sci. Eng. A* **384** 172
- [23] Yoshikawa M, Obata Y and Maegawa M 1995 *Appl. Phys. Lett.* **67** 694
- [24] Jian Z, Buscher H, Falter C, Ludwig W, Zhang K and Xie X 1996 *Appl. Phys. Lett.* **69** 200
- [25] Goldstein H F, Kim D S, Yu P Y and Bourne L C 1990 *Phys. Rev. B* **41** 7192
- [26] Xu J F, Ji W, Shen Z X, Tang S H, Ye X R, Jia D Z and Xin X Q 1999 *Solid State Chem.* **147** 516
- [27] Wang Z, Pischedda V, Saxena S K and Lazor P 2002 *Solid State Commun.* **121** 275
- [28] Dar M A, Ahsanulhaq Q, Kim Y S, Sohn J M, Kim W B and Shin H S 2009 *Appl. Surf. Sci.* **255** 6279
- [29] Balamurugan B and Mehta B R 2001 *Thin Solid Films* **396** 90
- [30] Dar M A, Kim Y S, Kim W B, Sohn J M and Shin H S 2008 *Appl. Surf. Sci.* **254** 7477
- [31] Othmani A, Plenet J C, Berstein E and Bouvier C 1994 *J. Cryst. Growth* **144** 141
- [32] Maji S K, Mukherjee N, Mondal A, Adhikary B and Karmakar B 2010 *Solid State Chem.* **183** 1900
- [33] Santra K, Sarka C K, Mukherjee M K and Cosh B 1992 *Thin Solid Films* **213** 226
- [34] Abdul Momin M, Roksana P, Jalal Uddin M, Arifuzzaman Khan G M and Momtazul Islam 2010 *J. Bangladesh Electron.* **10** 57